



Original article

New 2H-chromene-3-carboxamide derivatives: Design, synthesis and use as inhibitors of hMAO

Zhi-Xiang Pan^{a,1}, Xu He^{a,1}, Yan-Yan Chen^a, Wen-Jian Tang^a, Jing-Bo Shi^a, Yu-Lan Tang^a, Bao-An Song^b, Jun Li^a, Xin-Hua Liu^{a,b,c,*}^a School of Pharmacy, Anhui Medical University, Hefei 230032, PR China^b Key Laboratory of Green Pesticide and Agriculture Bioengineering, Ministry of Education, Guizhou University, Guiyang 550025, PR China^c State Key Laboratory of Pharmaceutical Biotechnology, Nanjing University, Nanjing 210093, PR China

ARTICLE INFO

Article history:

Received 10 January 2014

Received in revised form

8 March 2014

Accepted 21 April 2014

Available online 23 April 2014

Keywords:

Coumarin

Design

Synthesis

Inhibitors

hMAO-B

ABSTRACT

A series new 2H-chromene-3-carboxamide derivatives **4a–4t** were synthesized and evaluated as monoamine oxidase A and B (MAO-A and MAO-B) inhibitors. Among them, compound **4d** (IC₅₀ = 0.93 μM, IC₅₀ iproniazid = 7.80 μM) showed the most activity and higher MAO-B selectivity (64.5-fold vs. 1-fold) with respect to the MAO-A isoform. The active compound **4d** was also docked into the hMAO-B complex structure active site to determine the probable binding model. The results indicated that conserved residue CYS172 was important for ligand binding via hydrogen bond interaction, Pi–Pi interaction was found between the benzene-ring of compound **4d** and residue ILE199.

© 2014 Elsevier Masson SAS. All rights reserved.

1. Introduction

Monoamine oxidases (MAOs) are a protein family of flavin-containing amine oxidoreductases that play an important role in the regulation and metabolism of several neurotransmitters, and their inhibitors (MAOIs) could be useful in the treatment of psychiatric and neurological diseases [1,2]. Two isoforms namely as MAO-A and MAO-B have been identified based on their amino acid sequences, three-dimensional structures, substrate specificity, and inhibitor selectivity [3,4]. MAO-A has a higher affinity for serotonin and noradrenaline, while MAO-B preferentially deaminates phenylethylamine and benzylamine. Despite of these differences, dopamine and tyramine are common substrates for both isoforms. These properties determine the pharmacological interest of MAOIs. MAO-A inhibitors act as antidepressant and anti-anxiety agents, whereas MAO-B inhibitors are used alone or in combination to treat Alzheimer's and Parkinson's diseases [5,6]. Monoamine oxidase B (MAO-B) activity is also increased in association with gliosis, which

can result in high levels of H₂O₂ and oxidative free radicals which are a possible source of oxidative stress for vulnerable neurons affected by Alzheimer's disease (AD) [7]. On the other hand, rasagiline, a selective MAO-B inhibitor, has been reported to retard the further deterioration of cognitive functions, displaying neuro-protective activity [8]. Therefore, the researcher's interest in the rational design is to search for novel, selective and efficient MAO-B inhibitors in recent years.

Coumarins are a large family of compounds, of natural and synthetic origin, that display a variety of pharmacological properties. Recently, coumarins and their derivatives were extensively studied to their antioxidative and enzymatic inhibition properties. Numerous functionalized coumarins have been presented as potent MAO and/or AChE inhibitors and some of them have been proposed for treating AD [9–11].

Structure–activity relationship of recent research showed that substitution in position 3 of the coumarin nucleus modulated MAO-B inhibitory activity [12,13]. When introducing an arylamide group or an alkylamide group in that position (Fig. 1A, B), which could provide them with additional strong selectivity inhibitory activity toward hMAO-B [14].

Based on the X-ray structure MAO-B complex (2BYB, pdb), computer-generated docking molecular models of 2H-chromene-3-carboxamide derivatives were analyzed, when the position of the

* Corresponding author. School of Pharmacy, Anhui Medical University, Meishan Road 81, Hefei, 230032, PR China.

E-mail address: xhliuhx@163.com (X.-H. Liu).

¹ These authors contributed equally to this paper.

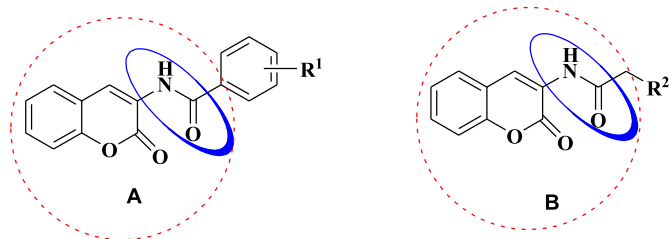


Fig. 1. General structures of the coumarin derivatives.

carbonyl group with interchangeable (Fig. 2C, D), which favor the formation of a stable binding (Fig. 2E), should help increase activity against MAO-B. Therefore, on the basis of rational design, we synthesis a series novel 2H-chromene-3-carboxamide derivatives used as selective and efficient MAO inhibitors.

2. Results and discussion

2.1. Chemistry

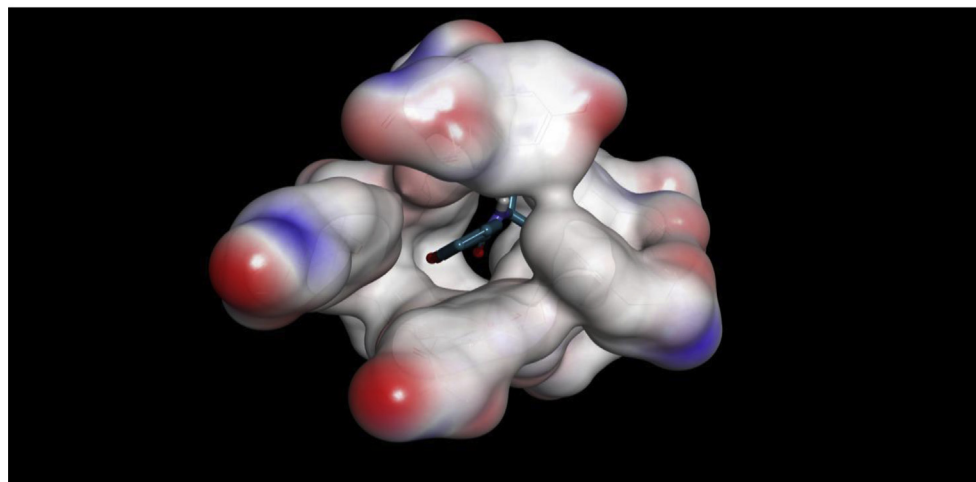
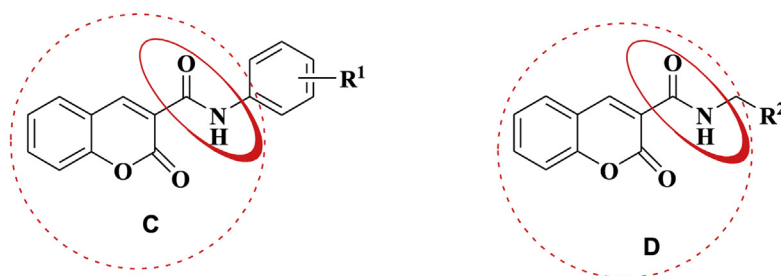
Coumarin title derivatives **4** were synthesized according to the protocol outlined in Scheme 1. Among them, compounds **1** (ethyl 2-oxo-2H-chromene-3-carboxylate) were prepared starting from a condensation of substituted-salicylaldehyde and the malonate. The reaction was performed in a dry schlenk tube, with piperidine as catalyst, ethanol as solvent, reflux for 2 h. Using simple sodium hydroxide and hydrochloric acid, proved to be an efficient alternative method for the synthesis of compounds **2** (2-oxo-2H-chromene-3-carboxylic acid). The key intermediate compounds **3** (2-oxo-2H-chromene-3-carbonyl chloride) were obtained through

the conventional thionyl chloride and compounds **2**, the reaction was performed in a dry schlenk tube, thionyl chloride also used as solvent, reflux for 1 h. The structure of compound **4j** was determined by X-ray crystallography. The molecular structure was shown in Fig. 3.

2.2. Inhibition of hMAO

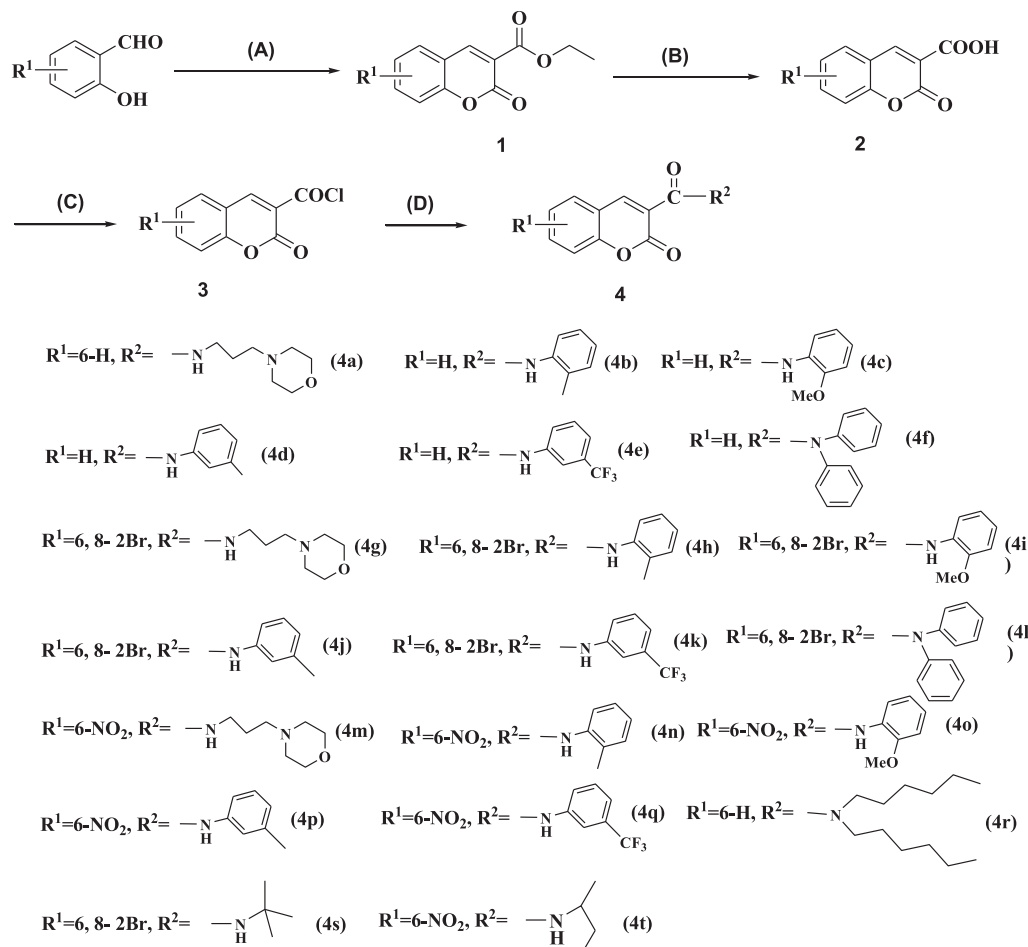
The potential effects of the synthesized compounds on hMAO activity were investigated by measuring their effects on the production of hydrogen peroxide (H_2O_2) from *p*-tyramine, using the Amplex Red MAO assay kit (Molecular Probes, Inc., Eugene, Oregon, USA) and MAO isoforms in microsomes prepared from insect cells infected with Recombinant baculovirus containing cDNA inserts for hMAO-A or hMAO-B. The inhibition of hMAO activity was evaluated using the general method described by L. Santana [15]. The test compounds did not show any interference with the reagents used for a biochemical assay. The results of hMAO-A and hMAO-B inhibition studies with title compounds were reported in Table 1 together with the MAO-A selectivity index.

It is obvious from the data that compounds **4b**, **4d**, **4e** and **4h** exhibited high activity against hMAO-B with IC_{50} values of 2.96 ± 0.62 , 0.93 ± 0.11 , 3.30 ± 0.21 and 4.68 ± 0.80 μM respectively, surpassing that of the positive control Iproniazide (7.80 ± 0.57). Among them, compound **4d** ($IC_{50} = 0.93$ μM) showed the most activity and higher hMAO-B selectivity (64.5-fold vs. 1-fold) with respect to the hMAO-A isoform. From the data presented in Table 1, it can be concluded that among all the synthetic compounds, two classifications can be made, one containing phenyl ring substitute on the N(H) moiety which include compounds **4b**, **4d**, **4e** and **4h**, and the other containing aliphatic chain substituent on the N(H) moiety which include compounds **4r**, **4s** and **4t** (see



E

Fig. 2. General design for the novel coumarin derivatives.



Scheme 1. Synthesis of title compounds **4**. Reagent and conditions: (A) $\text{CH}_2(\text{COOC}_2\text{H}_5)_2$, piperidine, reflux 2 h; (B) NaOH, reflux 3 h, HCl, pH = 2; (C) SO_2Cl_2 , reflux 1 h; (D) Substituted amines, CHCl_3 , DMAP, 25 °C, 2–3 h.

Scheme 1). We can see that compounds **4b**, **4d**, **4e** and **4h** showed obvious activity against hMAO with high selectivity toward hMAO-B, while for compounds **4r**, **4s** and **4t** with aliphatic chain substitute on the **N(H)** moiety, both activity and selectivity decreased. From the data presented in **Table 1**, we can easily summarize the structure–activity relationships of title compounds with different R^1 , R^2 substituents. First, title compounds (**4a**, **4d**, **4e**) containing unsubstituted coumarin ring ($R^1 = \text{H}$) show higher MAO-B activity than that compounds with substituted coumarin, such as compounds **4i**, **4j** ($R^1 = 6,8\text{-2Br}$), furthermore, compounds **4m**, **4o** ($R^1 = \text{-NO}_2$)

show even poor activity against MAO-B. Second, the substituent on the phenyl ring (for R^2) shows great influence on the activity, wherein, compounds with $-\text{CH}_3$ and $-\text{CF}_3$ are more conducive to the activity (**4a**, **4d**, **4e**), but compound with $-\text{OMe}$ does not contribute to activity (**4c**). This pointed out the direction for us to further optimize the structures of 2H-chromene-3-carboxamide derivatives as selective and potential hMAO inhibitors.

2.3. Molecular docking

In an effort to elucidate the mechanism by which the title compound exhibited strong inhibitory selective activity against hMAO-B and to establish an SAR based on our experimental studies, molecule docking of the compound **4d** into the ligand binding model site of MAO-B was performed on the binding model based on the MAO-B complex structure (2BYB.pdb) [3,16]. The binding model of compound **4d** with MAO-B complex was depicted in **Fig. 4**. The 2D and 3D pictures of binding were depicted in **Fig. 4A** and **B**. In order to reveal that the molecule was well filled in the active pocket, the enzyme surface was shown in **Fig. 4C**. Several bonding interactions anchoring compound **4d** to the active site tightly might explain its good inhibitory activity. There is a Pi-Pi interaction between the benzene-ring of compound **4d** and **N** atom of ILEA 199 with length of 2.68 Å. Another interaction is hydrogen bond between the backbone amino groups of CYSA 172 and carbonyl **O** atom of compound **4d**.

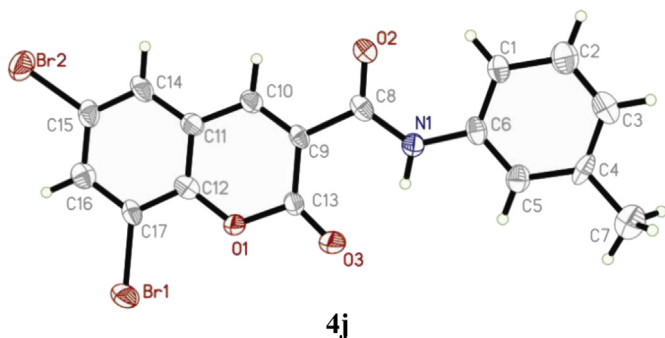


Fig. 3. ORTEP drawing of compounds **4j**.

Table 1
IC₅₀ values and hMAO-B selectivity index for the new compounds.^a

Compound	MAO-A (μM)	MAO-B (μM)	SI MAO-A ^c
4a	42.32 ± 1.21	13.46 ± 0.77	3.1 ^d
4b	^b	2.96 ± 0.62	20.3 ^d
4c	^b	35.40 ± 1.88	1.7 ^d
4d	^b	0.93 ± 0.11	64.5 ^d
4e	^b	3.30 ± 0.21	18.2 ^d
4f	^b	^b	–
4g	32.44 ± 0.75	10.56 ± 0.98	3.1 ^d
4h	^b	4.68 ± 0.80	12.8 ^d
4i	^b	20.17 ± 1.25	2.97 ^d
4j	^b	21.55 ± 1.47	2.78 ^d
4k	^b	7.09 ± 0.87	8.46 ^d
4l	^b	^b	–
4m	^b	46.07 ± 1.07	1.3 ^d
4n	^b	29.42 ± 1.78	2.0 ^d
4o	^b	50.03 ± 2.77	1.2 ^d
4p	^b	39.11 ± 1.36	1.5 ^d
4q	^b	22.80 ± 1.33	2.6 ^d
4r	14.20 ± 0.81	8.05 ± 0.64	1.8 ^d
4s	31.45 ± 1.09	14.71 ± 0.99	2.1 ^d
4t	37.53 ± 1.50	19.06 ± 2.00	1.97 ^d
Iproniazide	7.01 ± 0.61	7.80 ± 0.57	1.1

^a Each IC₅₀ value is the mean ± SEM from three experiments (*n* = 3).^b Inactive at 60 μM (highest concentration tested).^c SI MAO-B = [IC₅₀(MAO-A)]/[IC₅₀(MAO-B)].^d Values obtained under the assumption that the corresponding IC₅₀ against either MAO-A or MAO-B is the highest concentration tested (60 μM).

3. Conclusions

In summary, we designed and synthesized some 2H-chromene-3-carboxamide derivatives as selective and efficient MAO-B inhibitors, followed by chemical synthesis and biological evaluated for them. Among them, compound **4j** was determined by X-ray. Enzymatic assays revealed that compound **4d** exhibited strong selectivity inhibitory activity toward hMAO-B, more than 64-fold and 1-fold inhibition levels with respect to the MAO-A isoform. Furthermore, the binding mode of high active compound **4d** on the hMAO-B indicated that conserved residue CYS172 was important for ligand binding via hydrogen bond interactions. In brief, based on reasonable molecular design, compared with the SAR of previous studies [14], the advantages of this study were that we found more efficient hMAO-B inhibitor. These results are helpful in the rational design of more efficient and selective hMAO inhibitors in the future.

4. Experimental section

4.1. Chemistry

The reactions were monitored by thin layer chromatography (TLC) on Merck pre-coated silica GF254 plates. Melting points (uncorrected) were determined on a XT4MP apparatus (Taikang Corp., Beijing, China). ¹H NMR and ¹³C NMR spectra were collected on PX400 spectrometer at room temperature with TMS and solvent signals allotted as internal standards. Chemical shifts are reported in ppm (δ). Elemental analyses were performed on a CHN-O-Rapid instrument, and were within ±0.4% of the theoretical values. Mass spectra were performed on an Agilent 1260-6221 TOF mass spectrometer.

4.2. General procedure for the synthesis of title compounds **4**

To a solution of 2-oxo-2H-chromene-3-carbonyl chloride **3** (2 mmol) and DMAP (4-dimethylaminopyridine, 2 mmol) in chloroform (30 mL) at 10 °C was added dropwise substituted amines

(3.0 mmol) for 30 min. The reaction mixture was stirred at room temperature for 2–3 h and washed with 20 mL H₂O, 10 mL 1% NaHCO₃, respectively, then dried on anhydrous MgSO₄. The solvent was removed in vacuo and the crude residue was purified by chromatography on SiO₂ (acetone/petroleum, 4: 1, v/v) to give title compounds **4a–4t** as a colorless solid. Compounds **1–3** were prepared according to references [14,17].

4.2.1. **4a**: *N*-(3-morpholinopropyl)-2-oxo-2H-chromene-3-carboxamide

colorless crystals, yield, 81%; mp 216–217 °C; ¹H NMR (400 MHz, CDCl₃) δ 8.97 (s, 1H, –NH–), 8.90 (s, 1H, chromen C₄–H), 7.67 (dd, *J* = 15.8, 7.8 Hz, 2H, ArH), 7.38 (dd, *J* = 14.8, 7.8 Hz, 2H, ArH), 3.73 (t, *J* = 4.1 Hz, 4H), 3.54 (d, *J* = 6.5 Hz, 2H), 2.45 (t, *J* = 6.2 Hz, 6H), 1.83 (s, 1H), 1.80 (s, 1H). ¹³C NMR (101 MHz, DMSO-*d*₆) δ: 161.01, 160.36, 153.88, 147.41, 134.07, 130.27, 125.16, 119.08, 118.52, 116.16, 66.13, 56.17, 53.43, 37.84, 25.58. TOF-HRMS: *m/z* [M + H]⁺ calcd for C₁₇H₂₀N₂O₄: 316.35; found: 317.1479. Anal. calcd for C₁₇H₂₀N₂O₄: C, 64.54; H, 6.37; N, 8.86%. Found: C, 64.66; H, 6.51; N, 9.12%.

4.2.2. **4b**: 2-oxo-*N*-*o*-tolyl-2H-chromene-3-carboxamide

colorless crystals, yield, 84%; mp 230–231 °C; ¹H NMR (400 MHz, CDCl₃) δ 10.79 (s, 1H, –NH–), 9.05 (s, 1H, chromen C₄–H), 8.25 (d, *J* = 8.1 Hz, 1H, ArH), 7.75 (d, *J* = 7.8 Hz, 2H, ArH), 7.45 (d, *J* = 19.8 Hz, 2H, ArH), 7.28 (d, *J* = 10.3 Hz, 1H, ArH), 7.23 (s, 1H, ArH), 7.10 (t, *J* = 7.5 Hz, 1H, ArH), 2.43 (s, 3H, Me). ¹³C NMR (101 MHz, CDCl₃) δ: 162.01, 154.48, 149.00, 136.12, 134.36, 130.51, 129.96, 128.63, 126.75, 125.50, 125.00, 121.93, 118.86, 118.74, 116.75, 18.13. TOF-HRMS: *m/z* [M + H]⁺ calcd for C₁₇H₁₃NO₃: 279.29; found: 280.0969. Anal. calcd for C₁₇H₁₃NO₃: C, 73.11; H, 4.69; N, 5.02%. Found: C, 73.00; H, 4.44; N, 4.87%.

4.2.3. **4c**: *N*-(2-methoxyphenyl)-2-oxo-2H-chromene-3-carboxamide

colorless crystals, yield, 77%; mp 295–296 °C; ¹H NMR (400 MHz, CDCl₃) δ 11.30 (s, 1H, –NH–), 9.01 (s, 1H, chromen C₄–H), 8.55 (d, *J* = 8.0 Hz, 1H, ArH), 7.79–7.64 (m, 2H, ArH), 7.48–7.35 (m, 2H, ArH), 7.12 (t, *J* = 7.8 Hz, 1H, ArH), 7.01 (s, 1H, ArH), 6.94 (d, *J* = 8.1 Hz, 1H, ArH), 3.98 (s, 3H, OMe). ¹³C NMR (101 MHz, CDCl₃) δ 161.65, 159.28, 154.65, 149.27, 148.72, 134.29, 130.02, 127.83, 125.48, 124.70, 121.10, 120.79, 119.26, 118.89, 116.85, 110.35, 56.13. TOF-HRMS: *m/z* [M + H]⁺ calcd for C₁₇H₁₃NO₄: 295.29; found: 294.0913. Anal. calcd for C₁₇H₁₃NO₄: C, 69.15; H, 4.44; N, 4.74%. Found: C, 68.86; H, 4.41; N, 4.57%.

4.2.4. **4d**: 2-oxo-*N*-*m*-tolyl-2H-chromene-3-carboxamide

colorless crystals, yield, 75%; mp 207–208 °C; ¹H NMR (400 MHz, CDCl₃) δ 10.77 (s, 1H, –NH–), 9.02 (s, 1H, chromen C₄–H), 7.77–7.67 (m, 2H, ArH), 7.57 (s, 2H, ArH), 7.47–7.39 (m, 2H, ArH), 7.29 (s, 1H, ArH), 6.99 (d, *J* = 7.5 Hz, 1H, ArH), 2.39 (s, 3H, Me). ¹³C NMR (101 MHz, CDCl₃) δ: 161.97, 159.38, 154.62, 149.03, 139.12, 137.70, 134.48, 130.09, 129.04, 125.62, 125.81, 121.33, 118.87, 117.83, 116.87, 21.67. TOF-HRMS: *m/z* [M + H]⁺ calcd for C₁₇H₁₃NO₃: 279.29; found: 280.0969. Anal. calcd for C₁₇H₁₃NO₃: C, 73.11; H, 4.69; N, 5.02%. Found: C, 73.26; H, 4.77; N, 5.19%.

4.2.5. **4e**: 2-oxo-*N*-(3-(trifluoromethyl)phenyl)-2H-chromene-3-carboxamide

colorless crystals, yield, 71%; mp 213–214 °C; ¹H NMR (400 MHz, CDCl₃) δ 11.00 (s, 1H, –NH–), 9.03 (s, 1H, chromen C₄–H), 8.10 (s, 1H, ArH), 7.89 (d, *J* = 8.0 Hz, 1H, ArH), 7.74 (dd, *J* = 16.3, 8.1 Hz, 2H, ArH), 7.57–7.38 (m, 4H, ArH). ¹³C NMR (101 MHz, CDCl₃) δ: 162.01, 159.79, 154.69, 149.59, 138.30, 134.86, 130.23, 129.72, 125.79, 123.68, 121.50, 121.46, 118.75, 118.30, 117.49, 117.45, 116.96.

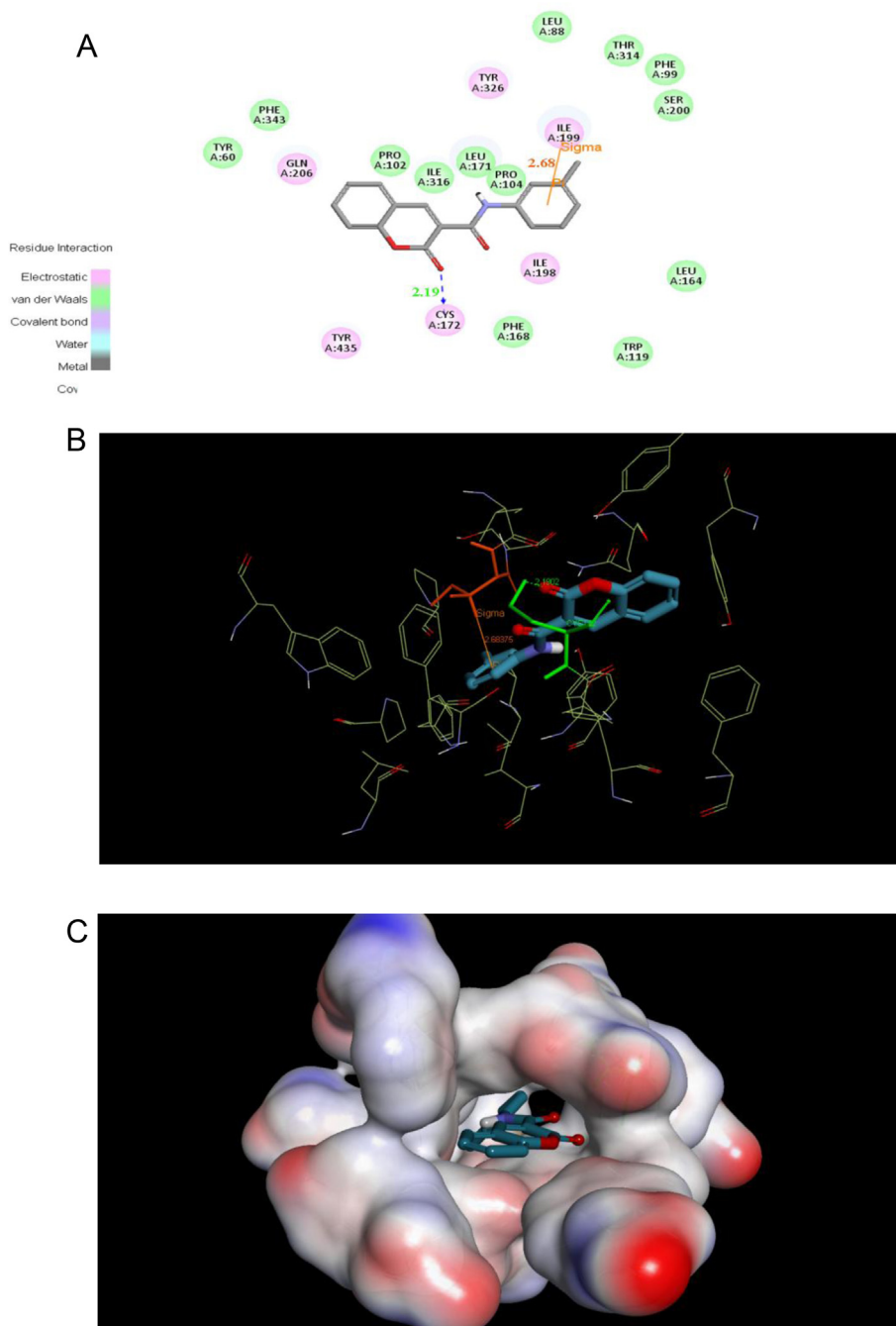


Fig. 4. Molecule docking of the compound **4d** into the ligand binding model site of MAO-B was performed on the binding model based on the MAO-B complex structure (2BYB.pdb). Panel A is a view into the active site cavity (A). The 2D picture of binding was depicted (B). The 3D picture of binding was depicted (C). In order to reveal that the molecule was well filled in the active pocket, the enzyme surface was shown.

TOF-HRMS: m/z $[M + Na]^+$ calcd for $C_{17}H_{10}F_3NO_3$: 333.26; found: 356.0505. Anal. calcd for $C_{17}H_{10}F_3NO_3$: C, 61.27; H, 3.02; N, 4.20%. Found: C, 61.15; H, 2.95; N, 4.08%.

4.2.6. **4f**: 2-oxo-*N,N*-diphenyl-2*H*-chromene-3-carboxamide

colorless crystals, yield, 68%; mp 243–244 °C; 1H NMR (400 MHz, $CDCl_3$) δ 7.95 (s, 1H, chromen C_4 -H), 7.55–7.47 (m, 2H, ArH), 7.39–7.26 (m, 9H, ArH), 7.23 (d, $J = 8.2$ Hz, 3H, ArH). TOF-HRMS: m/z $[M + H]^+$ calcd for $C_{22}H_{15}NO_3$: 341.36; found: 342.1119. Anal. calcd for $C_{22}H_{15}NO_3$: C, 77.41; H, 4.43; N, 4.10%. Found: C, 77.55; H, 4.38; N, 4.21%.

4.2.7. **4g**: 6,8-dibromo-*N*-(3-morpholinopropyl)-2-oxo-2*H*-chromene-3-carboxamide

colorless crystals, yield, 72%; mp 209–211 °C; 1H NMR (400 MHz, $CDCl_3$) δ 8.86 (s, 1H), 8.78 (s, 1H, -NH-), 7.99 (s, 1H, chromen C_4 -H), 7.76 (s, 1H, ArH), 3.74 (d, $J = 3.8$ Hz, 4H), 3.54 (d, $J = 6.4$ Hz, 2H), 2.47 (d, $J = 5.4$ Hz, 6H), 1.83 (d, $J = 6.7$ Hz, 2H). ^{13}C NMR (101 MHz, $CDCl_3$) δ : 160.66, 159.88, 146.70, 139.39, 131.15, 121.04, 120.58, 117.98, 111.35, 66.91, 56.73, 53.91, 38.68, 25.91. TOF-HRMS: m/z $[M + Na]^+$ calcd for $C_{17}H_{18}Br_2N_2O_4$: 474.14; found: 496.9527. Anal. calcd for $C_{17}H_{18}Br_2N_2O_4$: C, 43.06; H, 3.83; N, 5.91%. Found: C, 43.24; H, 4.02; N, 6.04%.

4.2.8. 4h: 6,8-dibromo-2-oxo-N-o-tolyl-2H-chromene-3-carboxamide

colorless crystals, yield, 78%; mp 235–236 °C; ¹H NMR (400 MHz, CDCl₃) δ 10.63 (s, 1H, –NH–), 8.91 (s, 1H, chromen C₄–H), 8.23 (d, J = 8.1 Hz, 1H, ArH), 8.02 (s, 1H, ArH), 7.81 (s, 1H, ArH), 7.28 (s, 1H, ArH), 7.23 (d, J = 7.3 Hz, 1H, ArH), 7.12 (d, J = 7.5 Hz, 1H, ArH), 2.41 (s, 3H, Me). ¹³C NMR (101 MHz, CDCl₃) δ: 160.72, 158.31, 150.29, 147.45, 139.69, 135.94, 131.28, 130.71, 128.67, 126.96, 125.41, 121.94, 120.99, 120.70, 118.25, 111.44, 18.14. TOF-HRMS: *m/z* [M + Na]⁺ calcd for C₁₇H₁₁Br₂NO₃: 437.08; found: 459.8988. Anal. calcd for C₁₇H₁₁Br₂NO₃: C, 46.71; H, 2.54; N, 3.20%. Found: C, 46.66; H, 2.79; N, 3.48%.

4.2.9. 4i: 6,8-dibromo-N-(2-methoxyphenyl)-2-oxo-2H-chromene-3-carboxamide

colorless crystals, yield, 81%; mp 237–238 °C; ¹H NMR (400 MHz, CDCl₃) δ 11.18 (s, 1H, –NH–), 8.87 (s, 1H, chromen C₄–H), 8.51 (d, J = 8.0 Hz, 1H, ArH), 8.01 (s, 1H, ArH), 7.80 (s, 1H, ArH), 7.13 (t, J = 7.8 Hz, 1H, ArH), 7.01 (t, J = 7.8 Hz, 1H, ArH), 6.94 (d, J = 8.1 Hz, 1H, ArH), 3.97 (s, 3H, OMe). TOF-HRMS: *m/z* [M + H]⁺ calcd for C₁₇H₁₁Br₂NO₄: 453.08; found: 451.9141. Anal. calcd for C₁₇H₁₁Br₂NO₄: C, 45.07; H, 2.45; N, 3.09%. Found: C, 44.98; H, 2.51; N, 3.32%.

4.2.10. 4j: 6,8-dibromo-2-oxo-N-m-tolyl-2H-chromene-3-carboxamide

colorless crystals, yield, 85%; mp 253–254 °C; ¹H NMR (400 MHz, CDCl₃) δ 10.59 (s, 1H, –NH–), 8.89 (s, 1H, chromen C₄–H), 8.02 (s, 1H, ArH), 7.81 (s, 1H, ArH), 7.54 (s, 2H, ArH), 7.28 (d, J = 7.8 Hz, 1H, ArH), 7.00 (d, J = 7.6 Hz, 1H, ArH), 2.39 (s, 3H, Me). ¹³C NMR (101 MHz, CDCl₃) δ: 160.47, 158.32, 150.35, 147.34, 139.68, 139.23, 137.35, 131.27, 129.10, 126.16, 121.37, 121.00, 120.60, 118.21, 117.89, 111.42, 21.66. TOF-HRMS: *m/z* [M + Na]⁺ calcd for C₁₇H₁₁Br₂NO₃: 437.08; found: 459.8998. Anal. calcd for C₁₇H₁₁Br₂NO₃: C, 46.71; H, 2.54; N, 3.20%. Found: C, 46.89; H, 2.59; N, 3.11%.

4.2.11. 4k: 6,8-dibromo-2-oxo-N-(3-(trifluoromethyl)phenyl)-2H-chromene-3-carboxamide

colorless crystals, yield, 80%; mp 198–199 °C; ¹H NMR (400 MHz, CDCl₃) δ 10.80 (s, 1H, –NH–), 8.90 (s, 1H, chromen C₄–H), 8.06 (d, J = 16.8 Hz, 2H, ArH), 7.93–7.77 (m, 2H, ArH), 7.62–7.37 (m, 2H, ArH). ¹³C NMR (101 MHz, DMSO-*d*₆) δ: 160.51, 158.74, 150.41, 147.91, 140.03, 137.94, 131.87, 131.87, 131.55, 129.80, 123.76, 121.86, 120.86, 120.05, 118.39, 117.57, 111.52. TOF-HRMS: *m/z* [M + Na]⁺ calcd for C₁₇H₈Br₂F₃NO₃: 491.05; found: 512.8715. Anal. calcd for C₁₇H₈Br₂F₃NO₃: C, 41.58; H, 1.64; N, 2.85%. Found: C, 41.33; H, 1.80; N, 3.02%.

4.2.12. 4l: 6,8-dibromo-2-oxo-N,N-diphenyl-2H-chromene-3-carboxamide

colorless crystals, yield, 69%; mp 241–242 °C; ¹H NMR (400 MHz, DMSO) δ 8.34 (s, 1H, chromen C₄–H), 8.17 (s, 1H, ArH), 7.99 (s, 1H, ArH), 7.33 (s, 10H, ArH). TOF-HRMS: *m/z* [M + H]⁺ calcd for C₂₂H₁₃Br₂NO₃: 499.05; found: 499.9308. Anal. calcd for C₂₂H₁₃Br₂NO₃: C, 52.94; H, 2.63; N, 2.81%. Found: C, 53.14; H, 2.45; N, 3.06%.

4.2.13. 4m: N-(3-morpholinopropyl)-6-nitro-2-oxo-2H-chromene-3-carboxamide

colorless crystals, yield, 72%; mp 180–181 °C; ¹H NMR (400 MHz, DMSO) δ 9.00 (s, 2H, –NH– and ArH), 8.75 (s, 1H, chromen C₄–H), 8.55–8.48 (m, 1H, ArH), 7.73 (d, J = 9.1 Hz, 1H, ArH), 3.59 (s, 4H), 3.42–3.36 (m, 2H), 2.35 (s, 6H), 1.78–1.61 (m, 2H). TOF-HRMS: *m/z* [M + H]⁺ calcd for C₁₇H₁₉N₃O₆: 361.35; found:

362.1345. Anal. calcd for C₁₇H₁₉N₃O₆: C, 56.51; H, 5.30; N, 11.63%. Found: C, 56.30; H, 5.47; N, 11.55%.

4.2.14. 4n: 6-nitro-2-oxo-N-o-tolyl-2H-chromene-3-carboxamide

colorless crystals, yield, 78%; mp 247–248 °C; ¹H NMR (400 MHz, DMSO) δ 10.54 (s, 1H, –NH–), 9.11 (s, 1H, chromen C₄–H), 8.67 (d, J = 2.3 Hz, 1H, ArH), 8.55 (dd, J = 9.2, 2.4 Hz, 1H, ArH), 8.22 (d, J = 8.1 Hz, 1H, ArH), 7.61 (d, J = 9.1 Hz, 1H, ArH), 7.29 (d, J = 7.7 Hz, 1H, ArH), 7.24 (s, 1H, ArH), 7.13 (t, J = 7.5 Hz, 1H, ArH), 2.42 (s, 3H, Me). ¹³C NMR (101 MHz, DMSO-*d*₆) δ 160.37, 158.88, 157.28, 146.97, 144.08, 135.97, 130.52, 128.46, 126.55, 126.21, 124.86, 121.58, 118.96, 117.88, 17.58. TOF-HRMS: *m/z* [M + Na]⁺ calcd for C₁₇H₁₂N₂O₅: 324.29; found: 347.0678. Anal. calcd for C₁₇H₁₂N₂O₅: C, 62.96; H, 3.73; N, 8.64%. Found: C, 63.02; H, 3.56; N, 8.43%.

4.2.15. 4o: N-(2-methoxyphenyl)-6-nitro-2-oxo-2H-chromene-3-carboxamide

colorless crystals, yield, 80%; mp 288–289 °C; ¹H NMR (400 MHz, DMSO) δ 11.09 (s, 1H, –NH–), 9.06 (s, 1H, chromen C₄–H), 8.65 (d, J = 2.4 Hz, 1H, ArH), 8.52 (d, J = 8.2 Hz, 2H, ArH), 7.58 (d, J = 9.1 Hz, 1H, ArH), 7.14 (t, J = 7.8 Hz, 1H, ArH), 7.02 (t, J = 7.8 Hz, 1H, ArH), 6.95 (d, J = 8.1 Hz, 1H, ArH), 3.98 (s, 3H, OMe). TOF-HRMS: *m/z* [M + H]⁺ calcd for C₁₇H₁₂N₂O₆: 340.29; found: 341.0754. Anal. calcd for C₁₇H₁₂N₂O₆: C, 60.00; H, 3.55; N, 8.23%. Found: C, 60.21; H, 3.70; N, 8.21%.

4.2.16. 4p: 6-nitro-2-oxo-N-m-tolyl-2H-chromene-3-carboxamide

colorless crystals, yield, 83%; mp 253–254 °C; ¹H NMR (400 MHz, DMSO) δ 10.53 (s, 1H, –NH–), 9.08 (s, 1H, chromen C₄–H), 8.66 (d, J = 2.5 Hz, 1H, ArH), 8.54 (dd, J = 9.1, 2.5 Hz, 1H, ArH), 7.57 (dd, J = 23.2, 9.1 Hz, 3H, ArH), 7.29 (d, J = 7.8 Hz, 1H, ArH), 7.01 (d, J = 7.6 Hz, 1H, ArH), 2.39 (s, 3H, Me). ¹³C NMR (101 MHz, DMSO-*d*₆) δ: 159.38, 159.35, 157.26, 145.87, 144.01, 138.41, 137.77, 128.93, 128.26, 125.99, 125.20, 122.44, 120.36, 118.86, 117.87, 117.05, 21.13. TOF-HRMS: *m/z* [M + H]⁺ calcd for C₁₇H₁₂N₂O₅: 324.29; found: 325.0826. Anal. calcd for C₁₇H₁₂N₂O₅: C, 62.96; H, 3.73; N, 8.64%. Found: C, 62.84; H, 3.77; N, 8.80%.

4.2.17. 4q: 6-nitro-2-oxo-N-(3-(trifluoromethyl)phenyl)-2H-chromene-3-carboxamide

colorless crystals, yield, 77%; mp 238–239 °C; ¹H NMR (400 MHz, CDCl₃) δ 10.73 (s, 1H, –NH–), 9.10 (s, 1H, chromen C₄–H), 8.68 (d, J = 2.6 Hz, 1H, ArH), 8.57 (dd, J = 9.1, 2.6 Hz, 1H, ArH), 8.07 (s, 1H, ArH), 7.90 (d, J = 8.0 Hz, 1H, ArH), 7.62 (d, J = 9.1 Hz, 1H, ArH), 7.52 (t, J = 8.0 Hz, 1H, ArH), 7.46 (d, J = 7.6 Hz, 1H, ArH). TOF-HRMS: *m/z* [M + Na]⁺ calcd for C₁₇H₉F₃N₂O₅: 378.26; found: 401.0346. Anal. calcd for C₁₇H₉F₃N₂O₅: C, 53.98; H, 2.40; N, 7.41%. Found: C, 54.05; H, 2.62; N, 7.33%.

4.2.18. 4r: N,N-dihexyl-2-oxo-2H-chromene-3-carboxamide

colorless crystals, yield, 75%; mp 197–198 °C; ¹H NMR (400 MHz, CDCl₃) δ 7.77 (s, 1H, chromen C₄–H), 7.61–7.49 (m, 2H, ArH), 7.39–7.28 (m, 2H, ArH), 3.47 (s, 2H), 3.24–3.15 (m, 2H), 1.72–1.61 (m, 2H), 1.55 (s, 2H), 1.35 (s, 6H), 1.23–1.14 (m, 6H), 0.90 (s, 3H), 0.79 (t, J = 6.6 Hz, 3H). ¹³C NMR (101 MHz, CDCl₃) δ: 157.33, 156.70, 144.43, 139.85, 128.81, 127.18, 124.19, 118.56, 118.21, 48.94, 45.12, 31.70, 31.46, 28.66, 27.33, 26.70, 26.45, 22.74, 22.60, 14.19, 14.06. TOF-HRMS: *m/z* [M + H]⁺ calcd for C₂₂H₃₁NO₃: 357.49; found: 358.2381. Anal. calcd for: C₂₂H₃₁NO₃: C, 73.91; H, 8.74; N, 3.92%. Found: C, 74.02; H, 8.55; N, 4.01%.

4.2.19. 4s: 6,8-dibromo-N-tert-butyl-2-oxo-2H-chromene-3-carboxamide

colorless crystals, yield, 82%; mp 184–185 °C; ¹H NMR (400 MHz, CDCl₃) δ 8.75 (s, 1H, –NH–), 8.61 (s, 1H, chromen C₄–H),

7.97 (s, 1H, ArH), 7.73 (s, 1H, ArH), 1.47 (s, 9H). ^{13}C NMR (101 MHz, CDCl_3) δ : 160.26, 159.35, 150.25, 146.19, 139.19, 131.01, 121.36, 121.06, 117.91, 111.24, 51.95, 28.75. TOF-HRMS: m/z [$\text{M} + \text{Na}$] $^+$ calcd for $\text{C}_{14}\text{H}_{13}\text{Br}_2\text{NO}_3$: 403.07; found: 424.9151. Anal. calcd for $\text{C}_{14}\text{H}_{13}\text{Br}_2\text{NO}_3$: C, 41.72; H, 3.25; N, 3.48%. Found: C, 41.89; H, 3.40; N, 3.62%.

4.2.20. **4t**: *N*-sec-butyl-6-nitro-2-oxo-2H-chromene-3-carboxamide

colorless crystals, yield, 71%; mp 205–206 °C; ^1H NMR (400 MHz, CDCl_3) δ 8.99 (s, 1H, $-\text{NH}-$), 8.62 (s, 1H, chromen C $_4$ -H), 8.54–8.37 (m, 2H, ArH), 7.55 (d, $J = 9.1$ Hz, 1H, ArH), 4.18–4.03 (m, 1H, ArH), 1.62 (d, $J = 7.4$ Hz, 2H), 1.25 (d, $J = 6.5$ Hz, 3H), 0.97 (t, $J = 7.4$ Hz, 3H). ^{13}C NMR (101 MHz, CDCl_3) δ : 160.18, 159.66, 157.52, 147.00, 144.69, 128.33, 125.53, 121.03, 118.84, 118.03, 47.62, 29.57, 20.36, 10.49. TOF-HRMS: m/z [$\text{M} + \text{Na}$] $^+$ calcd for $\text{C}_{14}\text{H}_{14}\text{N}_2\text{O}_5$: 290.27; found: 313.0793. Anal. calcd for $\text{C}_{14}\text{H}_{14}\text{N}_2\text{O}_5$: C, 57.93; H, 4.86; N, 9.65%. Found: C, 58.17; H, 5.01; N, 9.88%.

4.3. Crystallographic studies

X-ray single-crystal diffraction data for compound **4j** was collected on a Bruker SMART APEX CCD diffractometer at 296(2) K using MoK α radiation ($\lambda = 0.71073$ Å) by the ω scan mode. The program SAINT was used for integration of the diffraction profiles. The structures were solved by direct methods using the SHELXS program of the SHELXTL package and refined by full-matrix least-squares methods with SHELXL [18]. All non-hydrogen atoms of compound **4j** were refined with anisotropic thermal parameters. All hydrogen atoms were generated theoretically onto the parent atoms and refined isotropically with fixed thermal factors.

4.4. Crystal structure analysis

The structure of compound **4j** was determined by X-ray crystallography. Crystal data of **4j**: Colorless crystals, yield, 85%; mp 253–254 °C; $\text{C}_{17}\text{H}_{11}\text{Br}_2\text{NO}_3$, $M = 437$, monoclinic; $a = 16.632$ (3), $b = 14.417$ (3), $c = 23.258$ (3) (Å); $\alpha = 90$, $\beta = 95.659$ (17), $\gamma = 90$ (°), $V = 3163.6$ (11) nm^3 , $T = 293$ (2) K, $Z = 8$, $D_c = 1.835$ g/cm^3 , $F(000) = 1712$, Reflections collected/unique = 3113/1208, Data/restraints/parameters = 3113/0/209, Goodness of fit on $F^2 = 0.972$, Fine, $R_1 = 0.0718$, $wR(F^2) = 0.1913$.

4.5. hMAO activity assay

Enzymatic MAO-A and MAO-B activity of compounds was determined by a fluorimetric method. Briefly, 0.1 mL of sodium phosphate buffer (0.05 M, pH 7.4) containing various concentrations of the test drugs (new compounds or reference inhibitors). The appropriate amounts of recombinant hMAO-A or hMAO-B were adjusted to the same reaction velocity in the presence of both isoforms the same concentration of substrate: 165 pmol of *p*-tyramine/min (hMAO-A: 1.1 μg protein; specific activity: 150 nmol of *p*-tyramine oxidized per hydroxyphenylacetaldehyde/min/mg protein; hMAO-B: 7.5 μg protein; specific activity: 22 nmol of *p*-tyramine transformed/min/mg protein). The mixture was incubated for 15 min at 37 °C, placed in the dark fluorimeter chamber. After this incubation period, the reaction was started by adding 200 μM of 10-acetyl-3,7-dihydroxyphenoxazine reagent (Amplex Red assay kit, Molecular Probes, Inc., Eugene, OR), 1 U/mL horseradish peroxidase, and 1 mM *p*-tyramine. The production of H_2O_2 and, consequently, of resorufin, was quantified at 37 °C in a multi-detection microplate fluorescence reader based on the fluorescence generated (excitation, 545 nm, emission, 590 nm) over a 15 min period, during which the fluorescence increased linearly.

4.6. General procedure for molecular docking

Discovery Studio 2.5 (DS 2.5, Accelrys Software Inc., San Diego, California, USA). Crystal structure of telomerase (PDB entry 2BYB) was used as template. Hydrogen atoms were added to protein model. The added hydrogen atoms were minimized to have stable energy conformation and to also relax the conformation from close contacts. The active site was defined and sphere of 4 Å was generated around the active site pocket, with the active site pocket of BSAI model using C-DOCKER, a molecular dynamics (MD) simulated-annealing based algorithm module from DS 2.5. Random substrate conformations are generated using high-temperature MD. Candidate poses are then created using random rigid-body rotations followed by simulated annealing. The structure of protein, substrate were subjected to energy minimization using CHARMM forcefield as implemented in DS 2.5. A full potential final minimization was then used to refine the substrate poses. Based on C-DOCKER, energy docked conformation of the substrate was retrieved for postdocking analysis.

Acknowledgments

The authors wish to thank the National Natural Science Foundation of China, China (No. 21272008), Science and Technological Fund of Anhui Province for Outstanding Youth (1408085J04), China, Anhui Provincial Natural Science Foundation, China (1308085MH137), The Governor Fund Of Guizhou Province (20120037) and the Research Foundation of Doctor, Anhui Medical University, China (XJ201120, XJ201121).

Appendix A. Supplementary data

Supplementary data related to this article can be found at <http://dx.doi.org/10.1016/j.ejmech.2014.04.060>.

References

- [1] D.E. Edmondson, A. Mattevi, C. Binda, M. Li, F. Hubálek, *Current Medicinal Chemistry* 11 (2007) 1983–1993.
- [2] C. Binda, J. Wang, L. Pisani, C. Caccia, A. Carotti, P. Salvati, D.E. Edmondson, A. Mattevi, *Journal of Medicinal Chemistry* 50 (2007) 5848–5852.
- [3] L.D. Colibus, M. Li, C. Binda, A. Lustig, D.E. Edmondson, A. Mattevi, *Proceedings of the National Academy of Sciences of the United States of America* 102 (2005) 12684–12689.
- [4] C. Binda, F. Hubálek, D.E. Edmondson, A. Mattevi, *Nature Structural Biology* 9 (2002) 22–26.
- [5] J. Ma, M. Yoshimura, E. Yamashita, A. Nakagawa, A. Ito, T. Tsukihara, *Journal of Molecular Biology* 338 (2004) 103–114.
- [6] W. Weyler, Y.P. Hsu, X.O. Breakefield, *Pharmacology & Therapeutics* 47 (1990) 391–417.
- [7] J.L. Saura, J.M. Cesure, A.M. Da Prada, M. Chan-Palay, V. Huber, G. Löffler, J.G. Richard, *Neuroscience* 62 (1994) 15–30.
- [8] M.B.H. Youdim, O.B. Am, M. Yogeve-Falach, O. Weinreb, W. Maruyama, M. Naoi, T. Amit, *Journal of Neuroscience Research* 79 (2005) 172–179.
- [9] Y.R. Prasad, A.L. Rao, L. Prasoona, K. Murali, P.R. Kumar, *Bioorganic & Medicinal Chemistry Letters* 15 (2005) 5030–5034.
- [10] N. Gökhan-Kelekçi, S. Yabanoğlu, E. Küpeli, U. Salgin, Ö. Özgen, G. Uçar, E. Yeşilada, E. Kendi, A. Yeşilada, A.A. Bilgin, *Bioorganic & Medicinal Chemistry* 15 (2007) 5775–5786.
- [11] J. Venkatesan, B.N. Sinha, G. Ucar, A. Ercan, *Bioorganic & Medicinal Chemistry Letters* 18 (2008) 6362–6368.
- [12] M.J. Matos, D. Viña, E. Quezada, C. Picciau, G. Delogu, F. Orallo, L. Santana, E. Uriarte, *Bioorganic & Medicinal Chemistry Letters* 19 (2009) 3268–3270.
- [13] M.J. Matos, D. Viña, C. Picciau, F. Orallo, L. Santana, E. Uriarte, *Bioorganic & Medicinal Chemistry Letters* 19 (2009) 5053–5055.
- [14] D. Viña, M.J. Matos, M. Yañez, L. Santana, E. Uriarte, *Medicinal Chemistry Communications* 3 (2012) 213–218.
- [15] L. Santana, H. González-Díaz, E. Quezada, E. Uriarte, M. Yañez, D. Viña, F. Orallo, *Journal of Medicinal Chemistry* 51 (2008) 6740–6751.
- [16] E.M. Milczek, D. Bonivento, C. Binda, A. Mattevi, I. McDonald, D.E. Edmondson, *Journal of Medicinal Chemistry* 51 (2008) 8019–8026.
- [17] R. Satguru, J. McMahon, J.C. Padget, *Journal of Coatings Technology* 66 (1994) 47–55.
- [18] G.M. Sheldrick, SHELXTL-97, Program for Crystal Structure Solution and Refinement, University of Göttingen, Göttingen, Germany, 1997.